Blowdown of Pipelines Carrying Flashing Liquids

Yuri V. Fairuzov
Institute of Engineering, National University of Mexico, Mexico City 04510, Mexico

A mathematical model is developed to simulate a blowdown of a long pipeline conveying a flashing multicomponent mixture. The effect of the thermal capacitance of the pipe was incorporated into the model by employing a novel approach in the formulation of the energy equation for the fluid flow in the pipeline. The model was validated by comparison with previously published experimental data for the blowdown of a pipe containing a two-component mixture. A detailed study was performed to investigate the effect of heat transfer between the fluid flow and the pipe wall on the process of depressurization of a long pipeline. Numerical simulations were carried out to assess the effect of friction on the blowdown time. The results obtained lead to a better understanding of the blowdown phenomenon and can be used for predicting the consequences of controlled or uncontrolled releases of flashing liquids from long pipelines.

Introduction

The rupture of a pipeline containing a subcooled liquid at high pressure leads to its rapid depressurization (blowdown). The liquid flashes soon after its pressure reaches the saturation pressure corresponding to the fluid temperature and thereafter is discharged to the surroundings as a two-phase mixture. A study of the blowdown phenomenon is of interest in many engineering problems. Accurate prediction of critical two-phase flow is crucial in the simulation of the loss-of-coolant accident in a nuclear power plant. In the chemical and oil/gas industries, there is increasing concern about the safety of high-pressure pipelines that convey toxic or flammable substances. If the conveyed fluid is a flashing liquid, such as liquefied petroleum gas (LPG) or condensate (live oil), a rupture of the pipeline may lead to the formation of a vapor cloud. Knowledge of the flow characteristics at the rupture is necessary to establish boundary conditions (source terms) in models that describe the dispersion of the vapor cloud in the atmosphere.

The flashing process caused by the depressurization of a pipeline may result in a significant drop in fluid temperature. This is also a dangerous consequence of the blowdown, because the temperature of the pipe wall may be reduced to a temperature below the ductile–brittle transition temperature of the steel from which the pipeline is manufactured (Haque et al., 1990). In the oil/gas industry, controlled blowdowns are carried out to perform maintenance on the subsea transmission lines. The low temperatures generated within the fluid during the controlled blowdown may lead to the formation of hydrates and the blockage of the pipeline (Erickson and Mai, 1992).

Much of the past work has been concentrated on the modeling of blowdown from vessels or relatively short pipes. The focus has been on single-component systems (water/steam). A literature review of existing models, correlations, and computer codes is given by Lahey and Moody (1977), Riebold et al. (1981), and Jackson et al. (1981).

Blowdown from long pipelines has received comparatively little attention in the literature. Several methods and models have been proposed for simulating the gas pipeline blowdown (McKee, 1990; Goh, 1989). Botros et al. (1989) obtained an analytical solution of the problem by a linearization of the friction term in the momentum equation. However, this model cannot be applied to a two-phase blowdown. Morrow et al. (1980) presented a model for blowdown of a pipeline containing liquefied petroleum gas (LPG) without experimental validation. Grolmes et al. (1984) theoretically examined the blowdown of a pipeline containing a flashing one-component liquid. Their study is based the homogeneous equilibrium model (HEM) and the slip flow model of two-phase flow. Tam and Higgins (1990) developed a simple empirical model for predicting the mass flow rate out of the pipeline containing LPG. Richardson and Saville (1991) employed a quasi-steady-state model of two-phase flow for simulating blowdown of long pipelines carrying hydrocarbon mixtures and showed a limited model validation.

Recently, Chen et al. (1995a) extended Guerst's variational

principle for bubble flow (Guerst, 1986) to generalized multicomponent two-phase dispersions, and formulated a two-fluid model for single- or multicomponent vapor–liquid mixtures. In the second part of the article (Chen et al., 1995b), they proposed a simplified numerical method for solving two-phase, multicomponent flow equations and presented a detailed study of the blowdown from pipelines containing one- and two-component flashing mixtures.

All of the previously mentioned models for blowdown of long pipelines neglect the thermal capacitance of the pipe wall. Furthermore, most of these models assume that the fluid flow in the pipeline is adiabatic. The drop in fluid temperature during the blowdown process causes the transfer of heat from the pipe wall to the fluid flow. The ratio of wall thickness to the internal diameter for steel pipes employed in the transport of flashing liquids reaches 0.13, and a large amount of heat therefore may be transferred to the fluid during the depressurization of the pipeline.

The objective of this article is to improve the understanding of the blowdown phenomenon by taking into account the effect of heat transfer between the fluid flow and the pipe wall. A transient, multicomponent, two-phase pipe flow model is formulated and solved numerically. The effect of the thermal capacitance of the pipe wall is incorporated into the model by employing a new approach in the formulation of the energy conservation equation for the fluid flow in the pipeline. The model predictions are compared with previously published experimental results for the blowdown of a pipe containing LPG. The effect of the thermal capacitance of the pipe wall on the two-phase flow behavior during blowdown of a long pipeline is demonstrated. Numerical simulations are also carried out to assess the effect of friction on the blowdown time.

Description of the Depressurization Process

The process of pipeline depressurization can be divided into three stages: a depressurization wave propagation, a flashing boundary propagation, and a two-phase discharge.

Depressurization Wave Propagation. The rupture of the pipeline produces a rapid depressurization of the fluid (10^3–10^4 bar/s). The resultant depressurization wave propagates along the pipeline at the local sound speed. During a very short period of time, this propagation occurs in a single-phase liquid flow. The pressure at the intact end is unchanged from the initial pressure. The flow is choked at the ruptured end. After the expansion wave has reached the intact end, the fluid pressure in the pipeline is very close to the saturation pressure corresponding to the fluid temperature.

Flashing Boundary Propagation. The flashing boundary propagates along the pipeline, starting from the ruptured end. The depressurization process continues at a considerably reduced rate. When the pressure at the ruptured end has dropped by a sufficient value, the two-phase flow out of the pipeline ceases to be choked.

Two-Phase Discharge. After the flashing front has reached the intact end, flashing occurs within the whole pipeline. The flashing process causes constant changes of the flow patterns. The fluid temperature decreases due to the drop in the fluid pressure. The pipe wall is cooled by the fluid flowing through the pipeline.

It should be pointed out that the fluid pressure may reach a pressure far enough below its normal boiling pressure during the stage of the depressurization wave propagation. This phenomenon is commonly called the pressure undershoot (Alamgir and Lienhard, 1980). It results from a delayed bubble nucleation that may occur during a sudden expansion of a subcooled liquid. For long pipelines, the modeling of pressure undershoot is generally of no real practical significance because the time period during which the depressurization wave propagation occurs is short as compared to the total blowdown time.

Description of Pipeline Model

The pipeline blowdown model developed in this article consists of three parts: a hydrodynamic model, a break-flow model, and a heat-transfer model. A brief description of the major features of each of these models, including the major equations, is given in this section.

Hydrodynamic model

The hydrodynamic model describes the transient, multicomponent, two-phase flow in the pipeline. The model is based on the following assumptions: (1) the flow is one-dimensional; (2) the velocities of both phases are equal; and (3) the mixture is thermodynamic equilibrium with both phases at saturation conditions. The validity of these assumptions for the two-phase flashing flow in long pipes was demonstrated by many investigators (e.g., Wallis, 1980; Chen et al., 1995b). The lumped-parameter method (Delhaye, 1981; Grolmes, 1986; Solbrig and Gidaspow, 1976) is employed in the formulation of governing equations for the two-phase flow. The modeling approach consists of breaking a pipeline into a number of control volumes or nodes that are connected by junctions or flow paths. Mass and energy conservation equations are written for each node, and an approximate momentum equation is used to calculate flow rates through the flow paths.

The pipeline discretization used for the numerical simulation is illustrated in Figure 1. The governing equations for transient, multicomponent, two-phase pipe flow can be written as follows:

Conservation of Mass Equation.

$$\frac{dM_n}{dt} = \dot{m}_{k+1} - \dot{m}_k . \tag{1}$$

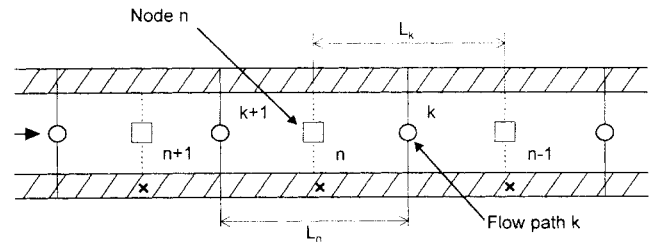

Figure 1. Discretization of a pipeline: □: center of node; ○: center of flow path; ×: pipe segment.

Momentum Equation.

$$\frac{d\dot{m}_k}{dt} = \frac{A}{L_k}(P_n - P_{n-1} - \Delta P_{F,n} - \Delta P_{F,n-1} - \Delta P_{M,k}), \quad (2)$$

where

$$L_k = \frac{L_n + L_{n-1}}{2};$$

$\Delta P_{F,n}$ is the pressure drop due to friction in node n; $\Delta P_{M,k}$ is pressure drop due to momentum change.

The two-phase pressure drop due to friction in node n is determined by

$$\Delta P_{F,n} = \Phi^2_{LO,n} \frac{f_n G_n^2 v_f}{2D} \times \frac{L_n}{2}, \quad (3)$$

where

$$G_n = \frac{\dot{m}_n}{A}. \quad (4)$$

The two-phase frictional multiplier is calculated using the correlation of MacAdams et al. (1942)

$$\Phi^2_{LO,n} = \left(1 + x\frac{(v_g - v_f)}{v_f}\right)_n \times \left(1 + x\frac{(\mu_f - \mu_g)}{\mu_f}\right)_n^{-1/4}. \quad (5)$$

The pressure drop due to changes in momentum flux for pipe flow is determined by

$$\Delta P_{M,k} = G_K^2(v_{n-1} - v_n). \quad (6)$$

Energy Equation.

$$\frac{d\left(U_n + \frac{M_n V_n^2}{2}\right)}{dt} = \dot{m}_{k+1}\left(h + \frac{V^2}{2}\right)_{n+1} - \dot{m}_k\left(h + \frac{V^2}{2}\right)_n + Q_n. \quad (7)$$

It should be noted the preceding equations require the knowledge of the mass flow rates and velocities at node centers. However, these variables are defined at node inlets and outlets (junctions). In order to complete the model formulation, the following auxiliary relationships are used:

$$\dot{m}_n = \frac{\dot{m}_k + \dot{m}_{k+1}}{2} \quad (8)$$

$$V_n = \frac{\dot{m}_n v_n}{A}. \quad (9)$$

For horizontal pipelines, the potential energy term in the energy equation can be neglected. The change of kinetic energy is accounted for in the model because it may be significant, in particular, in the beginning of the depressurization process when the flow is accelerated very rapidly.

In the preceding equations the thermodynamic properties of the multicomponent mixture are functions of pressure, temperature (or quality), and composition. The overall mixture composition is assumed to be constant along the pipeline. The liquid and vapor compositions change with pressure and temperature as a result of interfacial mass transfer. The thermodynamic and transport properties of the fluid are calculated using a computer program for predicting multicomponent vapor–liquid equilibria developed by Solorzano et al. (1996). The program is based on the Redlich–Kwong–Soave (RKS) and Peng–Robinson equations of state and allows the use of nine mixing rules. The RKS equation of state in combination with separate liquid-phase correlations (Reynolds, 1979) is used in this article. The standard error ($\sqrt{\Sigma \text{ error}^2/\text{number of points}}$) in property estimates is less than 2% (Solorzano et al., 1996).

At the intact end, either pressure or flow may be specified as a boundary condition. At the ruptured end, the exit flow is specified using a break-flow model, which is discussed in the next section. The flow is assumed to be at stagnation, initially. An exponential nodal spacing with the close spacing biased toward the ruptured end, where large gradients of flow parameters take place, is used. The length of a node is determined as follows:

$$L_n = L_0(F_n - F_{n-1}), \quad (10)$$

where

$$F_n = \left(\frac{n}{N}\right)^m \quad (11)$$

and L_o is the pipeline length.

Break-flow model

The break-flow model is used to predict the mass flow rate out of the pipeline. Both the choked and subsonic flow at the rupture are calculated. It is assumed that during blowdown through a full-bore rupture the flow undergoes an isentropic expansion with equal phasic velocities and temperatures.

To determine the choked flow at the rupture, the method for predicting critical two-phase flow proposed by Starkman et al. (1964) is extended here to multicomponent mixtures. The calculation procedure is based on seeking a maximum in the mass velocity by varying the static pressure at the discharge plane

$$G = [2(h_o - h)]^{1/2}/v. \quad (12)$$

Here the specific enthalpy and specific volume are expressed in terms of static pressure, quality (or vapor mass fraction) at the discharge plane, and overall mixture composition

$$h = h_f(p, z) + xh_{fg}(p, z) \quad (13)$$

$$v = v_f(p, z) + xv_{fg}(p, z). \quad (14)$$

The quality is determined along a constant entropy line

$$x = \frac{s_o - s_f(p,z)}{s_{fg}(p,z)}. \tag{15}$$

If the flow exiting the pipeline is subsonic, the static pressure at the discharge plane is equal to the ambient pressure, and the mass velocity is calculated from Eq. 12. For depressurization through a partial break, the mass velocity is multiplied by a discharge coefficient C_d in order to take friction at the ruptured end of the pipeline into account.

Heat-transfer model

The following simplifying assumptions are made in the analysis of heat transfer in the pipeline:

1. The fluid and pipe wall are in local thermal equilibrium. First, the thermal resistance of the two-phase flow is small since the heat transfer in the two-phase flow conditions is characterized by high heat-transfer coefficients (10^3–10^4 W/m^{2}K). Therefore, the temperature of the internal pipe surface is very close to the local fluid temperature. Second, in long pipelines there is sufficient time for thermal equilibrium within the pipe wall to be achieved. This can be demonstrated by a comparison of characteristic times of two processes, the fluid temperature decay and the transient cooling of the pipewall. The drop in fluid temperature is governed by the drop in the local fluid pressure; hence, the total time of pipeline depressurization may be used as an estimate for the characteristic time of the fluid temperature decay process. The characteristic time of the wall cooling process is the time that is required to reach the thermal equilibrium within the pipe wall after a sudden change in the heat-transfer conditions at the wall–fluid interface. It can be estimated with the use of the classic solution of the heat conduction equation for a hollow cylinder (Ozisik, 1993) and a correlation for two-phase forced-flow heat transfer (e.g., Chen, 1966). For blowdown of long pipelines, this time is of the order of 10^1–10^2 s, white the total blowdown time is 10^4–10^5 s, depending on the length and the diameter of the pipeline as well as the size of the rupture.

2. In the pipe wall, the heat transfer by conduction in the axial direction is negligible. The thermal gradients in axial direction are negligible in comparison with the radial gradients.

The pipe wall is divided into a number of isothermal segments, as shown in Figure 1. With the previously mentioned assumptions, the energy equation for a node and a pipe segment can be written as follows (see the Appendix):

This formulation of the energy equation is different from those used in prior models. The terms B_1 and B_2 in Eq. 16 (see the Appendix) incorporate the thermal capacitance of the pipe wall. Conjugate heat-transfer calculations are not required for predicting the heat transfer from the pipe wall to the fluid flow. This significantly reduces the computer time required for solving the problem.

The external heat flux is evaluated using Newton's law of cooling

$$Q_n = Ah_n(T_\infty - T_n), \tag{17}$$

where T_∞ is the ambient temperature.

Solution Method

The system of ordinary differential equations represented by Eqs. 1, 2, and 16 can be written in a vector form

$$\frac{dY}{dt} = F(t,Y), \tag{18}$$

where Y is the vector of dependent variables

$$Y = [M_1, M_2, \ldots, M_N, p_1, p_2, \ldots, p_N, \dot{m}_1, \dot{m}_2, \ldots, \dot{m}_K]^T. \tag{19}$$

The preceding system of ordinary differential equations with the initial and boundary conditions discussed earlier was solved by the Gear method (Gear, 1971). The total number of equations of the preceding system of equations is $2 \times N + K$. The maximum local error during the integration was kept under 0.1%. The partial derivatives of the specific volume and specific internal energy in Eqs. A6, A7, A13, and A14 were estimated numerically using the backward differences formula.

Results and Discussion

Model validation

The model validation was performed through comparison with the experimental data of Tam and Cowly (1984). They conducted a comprehensive series of experiments on pressurized LPG releases using two horizontal 100-m-long pipelines of internal diameters of 50 mm and 150 mm. The rupture of the pipeline was simulated by breaking a glass or graphite diaphragm installed at the spill end of the pipeline. Addi-

$$\frac{dp_n}{dt} = \frac{\left\{\dot{m}_{k+1}\left(h + \frac{V^2}{2}\right)_{n+1} - \dot{m}_k\left(h + \frac{V^2}{2}\right)_n - \left(u + \frac{V^2}{2} - \frac{B_2 v}{B_4}\right)_n (\dot{m}_{k+1} - \dot{m}_k) + Q_n - M_n\left(\frac{mv^2}{A^2}\right)_n \left[\frac{d\dot{m}_n}{dt} - \frac{\dot{m}_n}{M_n}(\dot{m}_{k+1} - \dot{m}_k)\right]\right\}}{M_n\left(B_1 - \frac{B_2 B_3}{B_4}\right)_n}. \tag{16}$$

tional orifice plates were used to investigate the effect of the size of the rupture on the release rate. The pipeline was suspended at 5-m intervals on hangers connected to load cells. The 20 load cells measured the mass of the fluid in the pipeline (mass inventory). The fluid temperatures and pressures were measured along the whole length of the pipeline by ten thermocouples with time constants of 50 ms and 10 pressure sensors with time constants of 0.5 ms, respectively. Void fraction was measured using the load cells as well as an independent method (neutron backscattering). Further details of this experiment can be found in the work of Chen et al. (1995b).

In this work, the experimental results for a full-bore rupture of the pipeline with a diameter of 150 mm are used to verify the model. The pipeline is made of commercial steel with an internal roughness characterized by a length scale of 0.05 mm. The pipeline is initially filled with pressurized LPG containing 95 mole% propane and 5 mole% butane. The initial pressure and temperature are 11.25 bar and 19.9°C, respectively. Variations of the measured inventory of the pipe, as well as the measured pressure, temperature, and void fraction at the closed and open ends of the pipeline, are used for validation. Pressures and temperatures were measured by the gauges and sensors that were 1.5 m from the closed end and 0.14 m from the open end. The void fraction was measured at a distance of 1.74 m from the closed end and 0.18 m from the opened end.

The assumptions made in the construction of the heat-transfer model are not valid for the pipeline used in this experiment. The thermal equilibrium between the pipe wall and fluid was not achieved because the blowdown time was too short (about 25 s). A rigorous conjugated heat-transfer model should be employed for a correct description of the transient heat transfer in the test pipeline. Nevertheless, the present heat-transfer model may also be used to describe approximately the heat-transfer phenomena occurring in the test pipeline during the depressurization process. It was assumed that a part of the wall adjacent to the internal surface of the pipe is in local thermal equilibrium with the fluid. Estimations show that the thickness of this "thermally penetrated" layer, averaged over the total blowdown time and the pipeline length, is about 1 mm.

The calculations were made using a 15-node pipeline model with $m = 1.2$. A further increase in the number of nodes did not have a significant effect on the model predictions. Calculations were performed on an HP Apollo Series 700 working station using a double-precision FORTRAN 77 code. Each calculation required approximately 1 h. The major part of CPU time was spent on the thermodynamic and phase-equilibrium calculations. The calculation for pure propane took less than 5 min.

The measured and predicted variations with time of inventory of the pipe, pressure, temperature, and void fraction at the closed and open ends of the pipeline are shown in Figures 2–6, respectively. The predicted results are the values at nodes adjoining the closed and open ends. As can be observed, there is good agreement between the values measured experimentally and those predicted by the present model. The model does not predict the small pressure undershoot in the beginning of the blowdown (Figure 3), because the stage of the depressurization wave propagation was not

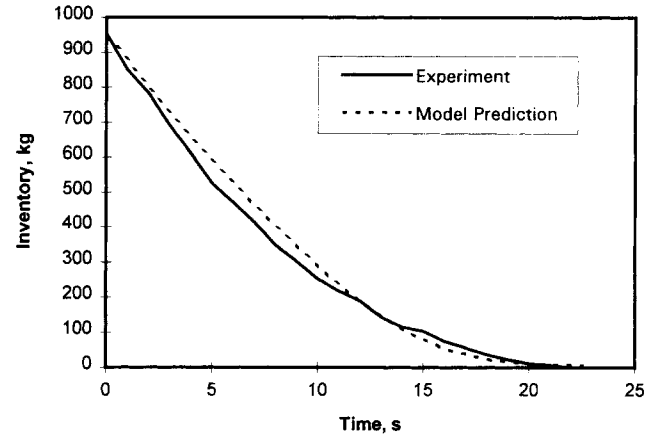

Figure 2. Variation of inventory of line with time.

simulated: the time of this process is very short (< 1 s). It was assumed that pressure drops instantly to the saturation pressure. Figure 3 shows that the model slightly overpredicts the rate of drop in pressure at the closed end of the pipeline. Chen et al. (1995b) also simulated the experiment of Tam and Cowly (1988) to validate their two-fluid model. They suggested that this discrepancy arises from (1) the uncertainty in the rupture mechanism, for example, some obstacle remains at the circumstance of the pipe after the breaking of the diaphragm, and (2) to the uncertainty in the roughness length scale. The present analysis indicates that this discrepancy may also result from an underestimation of the importance of the effect of heat transfer in the considered problem. If the flow is assumed adiabatic (legend "adiabatic flow," Figure 3), the pressure can be underpredicted significantly at the closed end.

There is also a discrepancy between the measured and predicted void fraction at the intact end (Figure 5). The present model overestimates the vapor generation rate during the first few seconds of the flashing process at the closed end of the pipeline. This discrepancy is attributed to the effects of thermal nonequilibrium. In the present model, the mixture is considered to be in thermal equilibrium, with both phases at saturation conditions. Such an equilibrium state can be achieved in the case of very slow transients. The homoge-

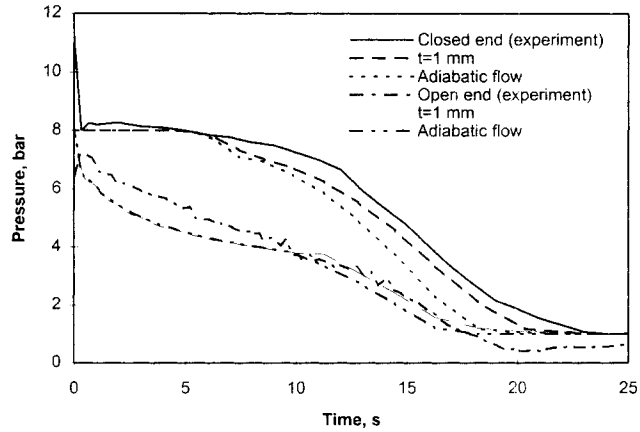

Figure 3. Variations of pressure at the closed and open ends of the line with time.

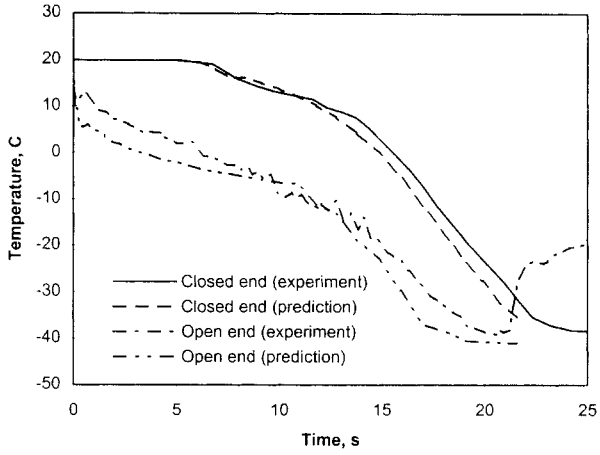

Figure 4. Variations of temperature at the closed and open ends of the line with time.

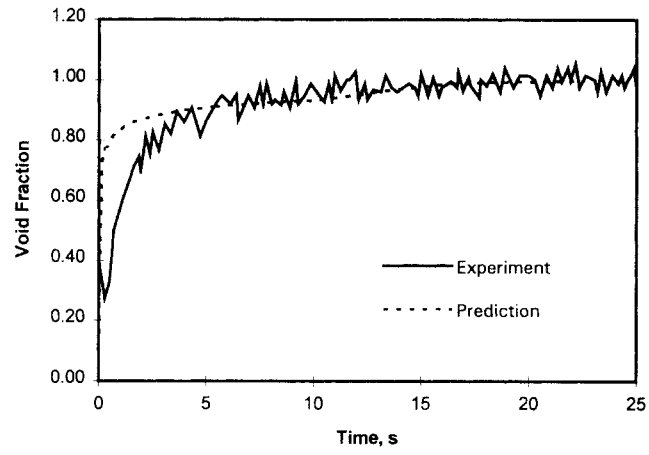

Figure 6. Variation of void fraction at open end of the line with time.

neous equilibrium model predicts the maximum possible vapor generation rate that is always larger than the actual rate. However, for blowdown of long pipelines with an L/D ratio of the order of 10^4–10^5, the blowdown time will be longer, and the thermal nonequilibrium effects will be less significant.

Effect of heat transfer

In order to demonstrate the effect of heat transfer on the two-phase flow behavior during blowdown of a long pipeline, a full-bore rupture of a horizontal pipeline of length 24 km and internal diameter 0.254 m (10 in.) was simulated. The pipeline is made of commercial steel. The pipe-wall thickness is of 0.01257 m (0.5 in.) The pipeline is filled with liquid propane. The initial pressure and temperature are 8.5 bar and 20°C, respectively. Calculations were carried out for four cases of thermal interaction between the pipe wall and the fluid flow: (1) the heat transfer between the pipe wall and the fluid flow is assumed to be negligible (legend "adiabatic flow"); (2) the pipeline is thermally isolated from the surroundings; however, the heat transfer between the pipe wall and the fluid flow is accounted for ($t/D = 0.05/h = 0$ W/m^{2}K); (3) it is assumed that the pipeline interchanges heat with the surroundings by natural convection characterized by a heat-transfer coefficient of 10 W/(m^{2}K), and the thermal capacitance of the pipe wall is negligible ($t = 0$); and (4) both the pipe thermal capacitance and the external heat transfer are taken into account ($t/D = 0.1$, $h = 10$ W/(m^{2}K)). As seen in Figure 7, the heat transfer has a relatively small effect on the mass flow rate out of the pipeline. This fact can be explained by examining the pressure and quality distributions along the pipeline (Figures 8 and 9). For clarity, results for only cases (1) and (2) are shown. The heat input to the flow decreases the rate of pressure drop in the pipeline (Figure 8). However, the pressure at the ruptured end drops very rapidly to the ambient pressure. According to Eq. 2, a higher pressure difference between the intact and ruptured end would result in an increase of the mass flow rate. However, the transfer of heat to the fluid flow also leads to a quicker evaporation of the liquid (Figure 9). The increase in quality results in an increase in friction pressure drop, Eqs. 3 and 5. Hence, the total effect of the heat transfer on the release rate is relatively small.

The correct prediction of the vapor release rate may be important in modeling vapor dispersion in the atmosphere. Figure 10 clearly illustrates the effect of heat transfer on the

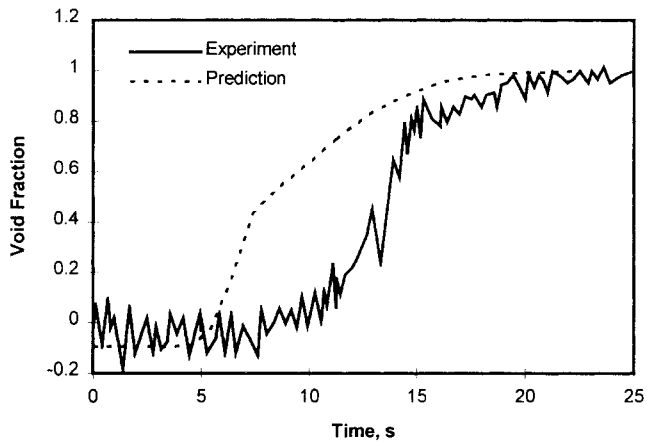

Figure 5. Variation of void fraction at the closed end of the line with time.

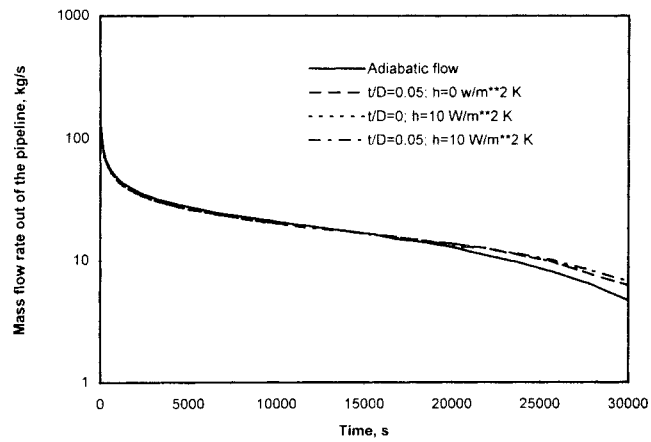

Figure 7. Mass flow rate out of the pipeline.

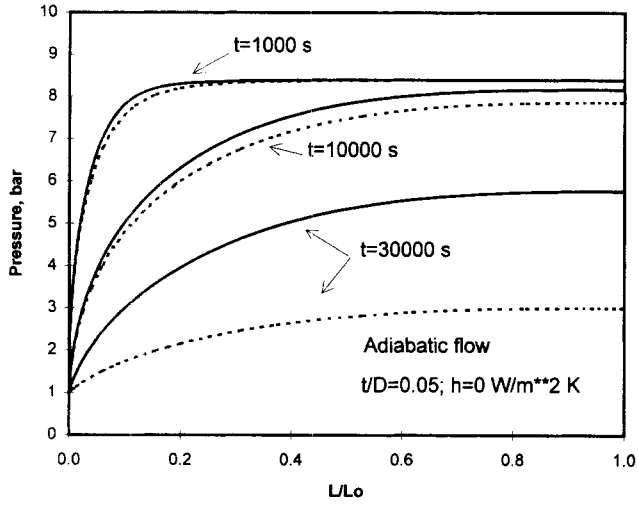

Figure 8. Transient pressure distributions in pipeline.

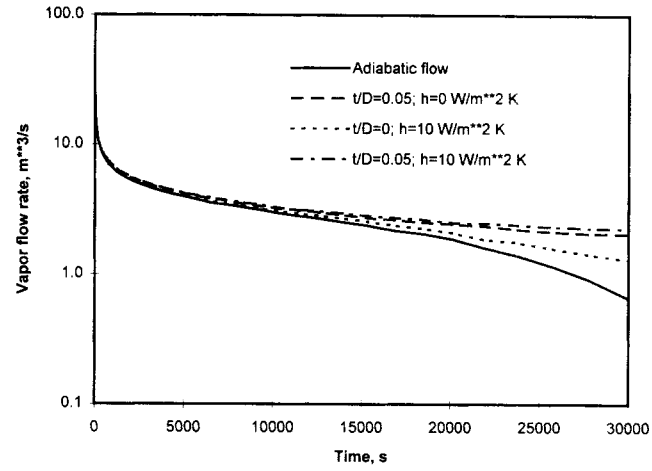

Figure 10. Effect of heat transfer on vapor release rate.

vapor release. The adiabatic-flow model underestimates the vapor flow rate out of the rupture, in particular, at late time of the transient.

Figure 11 shows the predicted temperature at the intact and ruptured ends of the pipeline for all previously mentioned cases. Both the wall thermal capacitance and the external convective heat transfer significantly affect the rate of temperature drop at the intact end. At the ruptured end, the fluid temperature drops rapidly to the saturation temperature corresponding to the ambient pressure.

Pipes of the same nominal size may have a different wall thickness. Figure 12 shows the effect of the wall thickness on pressure at the intact and ruptured ends of the pipeline at the end of the blowdown. Fluid pressures P_{ad} and P correspond to cases 1 and 2, respectively. The conditions of heat transfer within the pipeline do not affect the pressure at the ruptured end; it is equal to the ambient pressure because the flow is subsonic at the end of the transient. However, the intact end pressure greatly depends on the amount of heat transferred to the fluid flow. It is seen that ignoring the thermal capacitance of the pipe wall leads to a significant overestimation of the rate of pressure drop, even if the t/D ratio is small.

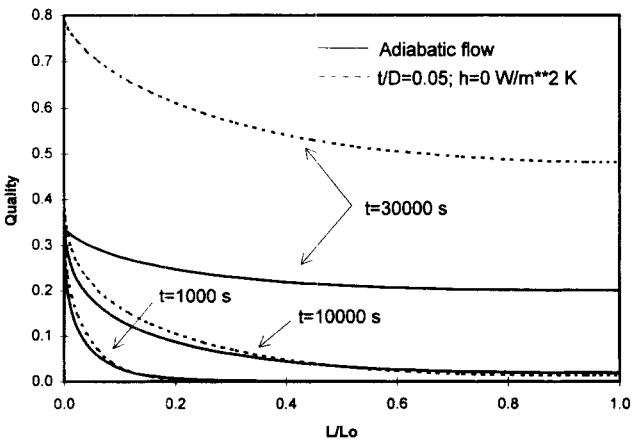

Figure 9. Transient quality distributions in pipeline.

Effect of friction

Generally, in the published work a single parameter, the fL/D ratio, is used for evaluating the effect of wall friction in pipes. However, in a study of blowdown phenomenon, the size of the rupture and the discharge coefficient should also be taken into consideration.

In order to fully demonstrate the effect of wall friction, some additional computations were performed using a 1-node pipeline model. This model neglects wall friction and assumes that stagnation conditions prevail inside the pipeline. Figure 13 shows the effect of two dimensionless parameters, fL/D and $(A_r C_d)/A$, on the total blowdown time. In these calculations it was assumed that the blowdown terminates when the mass of the fluid remaining in the pipeline is 1% of the initial mass of the fluid. The results are presented in terms of the ratio of the total blowdown time calculated from a 15-node model to that obtained from the 1-node model. It is seen that in the case of a full-bore rupture the effect of friction is significant even for relatively short pipes. The 1-node model significantly underpredicts the time over which the fluid is released from pipes having the fL/D ratio larger than

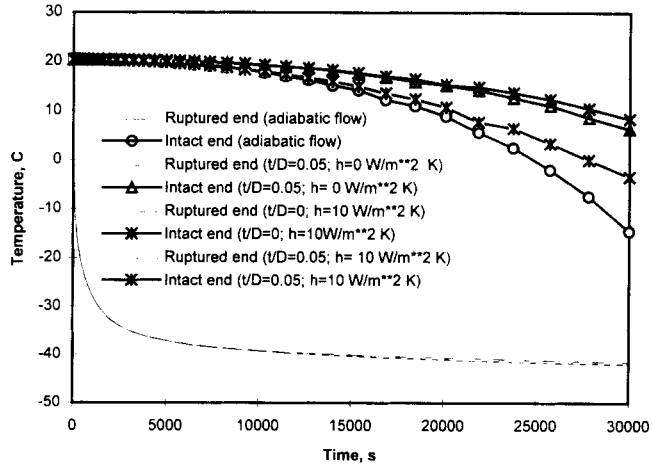

Figure 11. Effect of heat transfer on temperature at the intact and ruptured ends of the pipeline.

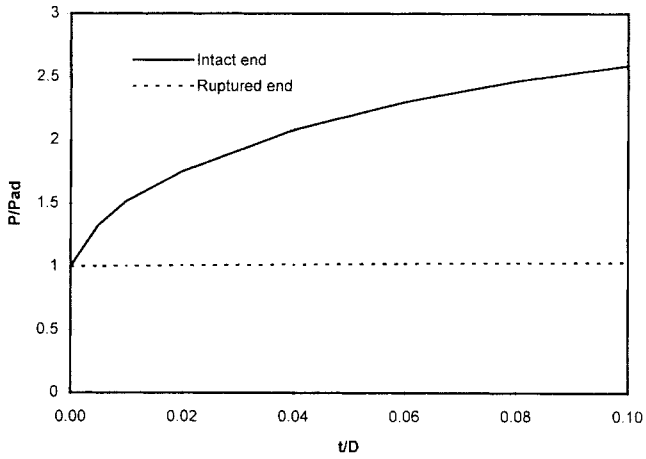

Figure 12. Effect of pipe thermal capacitance on the pressure at the intact and ruptured ends of the pipeline.

5. A partial break of the line—$(A_rC_d)/A = 0.1$—is characterized by a smaller release rate, and hence a smaller fluid velocity compared to the full-bore rupture. Therefore, the 1-node model can be applied for longer pipes.

Conclusions

1. A mathematical model for simulating the blowdown of a pipeline conveying a flashing multicomponent mixture was developed and solved numerically. The effect of the thermal capacitance of the pipe wall was incorporated into the model by employing a novel approach in the formulation of the energy conservation equation for the transient two-phase pipe flow. The model was validated by comparison with experimental data on pressurized LPG releases from a 100-m pipeline.

2. The effect of wall thickness on two-phase flow parameters during pipeline blowdown was demonstrated. It was found that the transfer of heat from the pipe wall to the fluid flow results in a significant decrease in the rate of pressure and temperature drop in the pipeline and in an increase in the vapor release rate. The effect of the heat transfer on the mass flow rate out of the pipeline is relatively small.

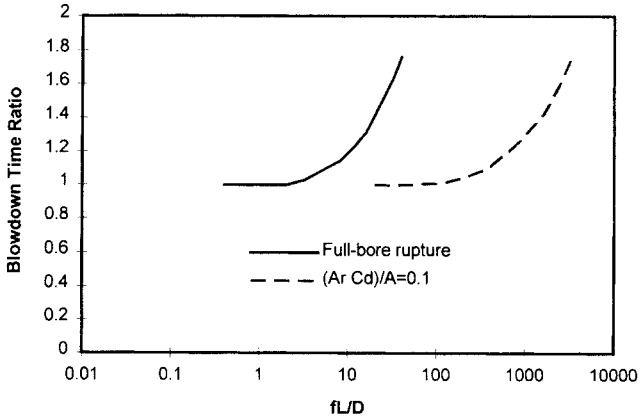

Figure 13. Effect of friction on the blowdown time.

3. The effect of friction can be estimated using two dimensionless parameters, namely fL/D and A_rC_d/A. Friction can be neglected for very short pipes ($fL/D < 5$). For longer pipes, the ignoring of wall friction results in an underestimation of the blowdown time.

4. The study revealed that the thermal capacitance of the pipe wall has a significant influence on the two-phase flow behavior and should not be neglected in the analysis of blowdown of long pipelines containing flashing liquids.

5. The results obtained in this article lead to a better understanding of the blowdown phenomenon and can be used in the prediction of the consequences of controlled or uncontrolled releases of flashing liquids from long pipelines.

Acknowledgments

This research was supported by DGAPA-UNAM under Grant No. IN-1055396 and by Mexican Petroleum Institute under Grant No. FJES-IV-96.

Notation

A = area
D = pipe internal diameter
G = mass velocity
f = friction factor
h = specific enthalpy; heat-transfer coefficient
M = mass
N = total number of nodes
K = total number of flow paths
$\dot{m}$ = mass flow rate
p = pressure
Q = external heat flux
t = time; pipe-wall thickness
U = internal energy
u = specific internal energy
x = quality
v = specific volume
V = fluid velocity
z = vector of overall mixture composition
μ = viscosity

Subscripts

f = liquid
fg = difference between liquid and vapor properties
g = vapor
n = node n
k = flow path k
m = two-phase mixture
r = rupture
w = pipe wall
o = stagnation properties

Literature Cited

Alamgir, Md., and J. H. Leinhard, "Correlation of Pressure Undershoot during Hot-Water Depressurization," *J. Heat Transfer*, **103**, 52 (1981).

Botros, K. K., W. M. Jungowski, and M. H. Weiss, "Models and Methods of Simulating Gas Pipeline Blowdown," *Can. J. Chem. Eng.*, **67** (1989).

Chen, J. C., "Correlation for Boiling Heat Transfer to Saturated Liquids in Convective Flow," *Int. Eng. Chem. Process Des. Dev.*, **5**, 322 (1966).

Chen, J. R., S. M. Richardson, and G. Saville, "Modelling of Two-Phase Blowdown from Pipelines—I. A Hyperbolic Model Based on Variational Principles," *Chem. Eng. Sci.*, **50**, 695 (1995a).

Chen, J. R., S. M. Richardson, and G. Saville, "Modelling of Two-Phase Blowdown from Pipelines—II. A Simplified Numerical Method for Multi-Component Mixtures," *Chem. Eng. Sci.*, **50**, 2173 (1995b).

Delhaye, J. M., "Basic Equations for Two-Phase Flow-Modeling," *Two-Phase Flow and Heat Transfer in the Power and Process Industries*, A. E. Bergles, J. G. Collier, J. M. Delhaye, G. F. Hewitt, and F. Mayinger, eds., Hemisphere, Washington, p. 40 (1981).
Erickson, D. D., and M. C. Mai, "A Transient Multiphase Temperature Prediction Program," *Proc. of 67th Annual Conference and Exhibition of the Society of Petroleum Engineers*, Washington, DC, p. 251 (Oct. 4–7, 1992).
Gear, C. W., *Numerical Initial Value Problems in Ordinary Differential Equations*, Prentice-Hall, Englewood Cliffs, NJ (1971).
Goh, C. B., "Estimation of Flowrate Through a Ruptured Natural Gas Pipe," *Int. J. Heat Fluid Flow*, **10**, 173 (1989).
Grolmes, M. A., J. C. Leung, and H. K. Fauske, "Transient Two-Phase Flow Discharge of Flashing Liquids Following a Break in Long Transmission Pipeline," *Multi-Phase Flow and Heat Transfer III, Part A: Fundamentals*, T. N. Veziroglu and A. E. Bergles, eds., Elsevier, Amsterdam, p. 567 (1984).
Geurst, J. A., "Variational Principles and Two-Fluid Hydrodynamics of Bubbly Liquid/Gas Mixtures," *Physica*, **135A**, 455 (1986).
Haque, A., S. M. Richardson, G. Saville, and G. Chamberlain, "Rapid Depressurization of Pressure Vessels," *J. Loss Prev. Process Ind.*, **3**, 4 (1990).
Jackson, J. F., D. R. Liles, V. H. Ransom, and L. J. Ybarrondo, "LWR System Safety Analysis," *Nuclear Reactor Safety Heat Transfer*, O. C. Jones, ed., Hemisphere, Washington, p. 415 (1981).
Lahey, R. T., and F. J. Moody, *The Thermal-Hydraulics of a Boiling Water Nuclear Reactor*, American Nuclear Society, LaGrange Park, IL (1977).
MacAdams, W. H., "Vaporisation Inside Horizontal Tubes. II. Benzene-Oil Mixture," *Trans. ASME*, **64**, 193 (1942).
McKee, R. J., "Simplified Blowdown Calculations," *Pipeline Gas J.*, 40 (April 1990).
Morrow, T. B., J. A. Lock, R. L. Bass, and F. T. Dodge, "Pipe Line Break Flow Model," SwRI Project No. 02-5953, Final Rep. (1980).
Ozisik, M. N., *Heat Conduction*, 2nd ed., Wiley, New York (1993).
Reibold, W. L., M. Reocreux, and O. C. Jones, "Blowdown Phase," *Nuclear Reactor Safety Heat Transfer*, O. C. Jones, ed., Hemisphere, Washington, p. 415 (1981).
Reynolds, W. C., "Thermodynamic Properties in SI," Stanford University, Stanford, CA (1979).
Richardson, S. M., and G. Saville, "Blowdown of Pipelines," *Proc. Offshore Europe 91*, **369**, Aberdeen, U.K. (Sept. 3-6, 1991).
Solbrig, C. W., and D. Gidaspow, "Equilibrium Homogeneous Transient Two-Phase Flow," *Two-Phase Flows and Heat Transfer*, Vol. III, S. Kakac and T. N. Veziroglu, eds., *Proc. of NATO Advanced Study Institute*, Istanbul, Turkey, p. 1171 (1976).
Solorzano, M., F. Barragan, and E. R. Bazua, "Comparative Study of Mixing Rules for Cublic Equations of State in the Prediction of Multicomponent Vapor-Liquid Equilibria," *Phase Equilibria*, **122**, 99 (1996).
Starkman, E. S., V. E. Schrock, K. F. Neusen, and D. J. Maneely, "Expansion of a Very Low Quality Two-Phase Fluid Through a Convergent-Divergent Nozzle," *J. Basic Eng. Trans. ASME*, Ser. D, **86**, 247 (1964).
Tam, V. H. Y., and L. T. Cowley, "Consequences of Pressurized LPG Releases: The Isle of Grain Full-Scale Experiments," *Proc. GASTECH 88 (13th Int. LNG/LPG Conf.)*, Kuala Lumpur, p. 2 (1988).
Tam, V. H. Y., and R. B. Higgins, "Simple Transient Release Models of Pressurized Liquid Petroleum Gas from Pipelines," *J. Hazard. Mater.*, **25**, 193 (1990).
Wallis, G. B., "Critical Two-Phase Flow," *Int. J. Multiphase Flow*, **6**, 97 (1981).

Appendix

The energy equation for a node and a pipe segment can be written as

$$\frac{d\left(U_n + \frac{M_n V_n^2}{2} + U_{w,n}\right)}{dt} = \dot{m}_{k+1}\left(h + \frac{V^2}{2}\right)_{n+1} - \dot{m}_k\left(h + \frac{V^2}{2}\right)_n + Q_n. \quad \text{(A1)}$$

The specific internal energy of a two-phase multicomponent mixture of a constant composition at a node n can be expressed as a function of p_n and x_n

$$u_n = u_{f,n} + x_n u_{fg,n}, \quad \text{(A2)}$$

where $u_{f,n}$ and $u_{fg,n}$ are also functions of p_n and x_n. Noting that

$$dU_{w,n} = M_{w,n} c_w dT, \quad \text{(A3)}$$

and substituting Eqs. A2 and A3 into Eq. A1 gives

$$B_1 \frac{dp_n}{dt} + B_2 \frac{dx_n}{dt} = \frac{\dot{m}_{k+1}\left(h + \frac{V^2}{2}\right)_{n+1} - \dot{m}_k\left(h + \frac{V^2}{2}\right)_n - \left(u + \frac{V^2}{2}\right)_n (\dot{m}_{k+1} - \dot{m}_k) + Q_n - M_n \frac{d}{dt}\left(\frac{V^2}{2}\right)_n}{M_n}, \quad \text{(A4)}$$

where

$$B_1 = \left[\left(\frac{\partial u_f}{\partial p}\right)_x + \frac{M_w c_w}{M}\left(\frac{\partial T}{\partial p}\right)_x + x\left(\frac{\partial u_{fg}}{\partial p}\right)_x\right]_n \quad \text{(A5)}$$

$$B_2 = \left[\left(\frac{\partial u_f}{\partial x}\right)_p + \frac{M_w c_w}{M}\left(\frac{\partial T}{\partial x}\right)_p + x\left(\frac{\partial u_{fg}}{\partial x}\right)_p + u_{fg}\right]_n. \quad \text{(A6)}$$

The volume of a node is constant, thus

$$\frac{d(M_n v_n)}{dt} = 0. \quad \text{(A7)}$$

Substituting Eq. 1 into Eq. A7 leads to

$$\frac{dv_n}{dt} = -\frac{v_n}{M_n}(\dot{m}_{k+1} - \dot{m}_k). \quad \text{(A8)}$$

Again, the specific volume of a two-phase multicomponent mixture of a constant composition can be expressed as a function of p_n and x_n

$$v_n = v_{f,n} + x_n v_{fg,n}, \quad \text{(A9)}$$

where $v_{f,n}$ and $v_{fg,n}$ are also functions of p_n and x_n. Equation A9 can be substituted into Eq. A8 to yield an expression for the dx_n/dt term as

$$\frac{dx_n}{dt} = -\frac{v_n}{B_4 \cdot M_n}(\dot{m}_{k+1} - \dot{m}_k) - \frac{B_3}{B_4}\frac{dp_n}{dt}, \qquad \text{(A10)}$$

where

$$B_3 = \left[\left(\frac{\partial v_f}{\partial p}\right)_x + x\left(\frac{\partial v_{fg}}{\partial p}\right)_x\right]_n \qquad \text{(A11)}$$

$$B_4 = \left[\left(\frac{\partial v_f}{\partial x}\right)_p + x\left(\frac{\partial v_{fg}}{\partial x}\right)_p + v_{fg}\right]_n. \qquad \text{(A12)}$$

The rate of change of kinetic energy at a node n can be expressed as

$$\frac{d}{dt}\left(\frac{V^2}{2}\right)_n = \left(\frac{\dot{m}v}{A}\right)_n \frac{d}{dt}\left(\frac{\dot{m}v}{A}\right)_n. \qquad \text{(A13)}$$

Differentiating the last term in Eq. A13 and substituting Eq. 1 into the resulting equation yields

$$\frac{d}{dt}\left(\frac{V^2}{2}\right)_n = \left(\frac{\dot{m}v^2}{A^2}\right)_n \left[\frac{d\dot{m}_n}{dt} - \frac{\dot{m}_n}{M_n}(\dot{m}_{k+1} - \dot{m}_k)\right]. \qquad \text{(A14)}$$

Finally, substituting Eqs. A10 and A14 into Eq. A2, after some rearrangement of terms, leads to

$$\frac{dp_n}{dt} = \frac{\left\{\dot{m}_{k+1}\left(h + \frac{V^2}{2}\right)_{n+1} - \dot{m}_k\left(h + \frac{V^2}{2}\right)_n - \left(u + \frac{V^2}{2} - \frac{B_2 v}{B_4}\right)_n (\dot{m}_{k+1} - \dot{m}_k) + Q_n - M_n\left(\frac{mv^2}{A^2}\right)_n\left[\frac{d\dot{m}_n}{dt} - \frac{\dot{m}_n}{M_n}(\dot{m}_{k+1} - \dot{m}_k)\right]\right\}}{M_n\left(B_1 - \frac{B_2 B_3}{B_4}\right)_n}. \qquad \text{(A15)}$$

Manuscript received Oct. 3, 1996, and revision received June 9, 1997.